



Supplementary information

<https://doi.org/10.1038/s43588-024-00738-w>

An integrative data-driven model simulating *C. elegans* brain, body and environment interactions

In the format provided by the
authors and unedited

Supplementary Information

Supplementary Table 1. Ion Channel Models

Ion Channel	Dynamic Model
SHL1	$m_{\text{SHL1},\infty}(V) = \frac{1}{1 + e^{\frac{-(V-V_{0.5})}{k_a}}}$ $\tau_{m_{\text{SHL1}}}(V) = \frac{a}{e^{\frac{-(V-b)}{c}} + e^{\frac{(V-d)}{\tilde{e}}}} + f$ $h_{\text{SHL1},\infty}^f(V) = h_{\text{SHL1},\infty}^s(V) = \frac{1}{1 + e^{\frac{(V-V_{0.5})}{k_i}}}$ $\tau_{h_{\text{SHL1}}}^f(V) = \tau_{h_{\text{SHL1}}}^s(V) = \frac{a}{1 + e^{\frac{(V-b)}{c}}} + d$ $I_{\text{SHL1}} = \bar{g}_{\text{SHL1}} \cdot m_{\text{SHL1}}^3 \cdot (0.7h_{\text{SHL1}}^f + 0.3h_{\text{SHL1}}^s) \cdot (V - V_K)$
KVS1	$m_{\text{KVS1},\infty}(V) = \frac{1}{1 + e^{\frac{-(V-V_{0.5})}{k_a}}}$ $h_{\text{KVS1},\infty}(V) = \frac{1}{1 + e^{\frac{(V-V_{0.5})}{k_i}}}$ $\tau_{m_{\text{KVS1}}}(V) = \tau_{h_{\text{KVS1}}}(V) = \frac{a}{1 + e^{\frac{(V-b)}{c}}} + d$ $I_{\text{KVS1}} = \bar{g}_{\text{KVS1}} \cdot m_{\text{KVS1}} \cdot h_{\text{KVS1}} \cdot (V - V_K)$
SHK1	$m_{\text{SHK1},\infty}(V) = \frac{1}{1 + e^{\frac{-(V-V_{0.5})}{k_a}}}$ $\tau_{m_{\text{SHK1}}}(V) = \frac{a}{e^{\frac{-(V-b)}{c}} + e^{\frac{(V-d)}{\tilde{e}}}} + f$ $h_{\text{SHK1},\infty}(V) = \frac{1}{1 + e^{\frac{(V-V_{0.5})}{k_i}}}$ $\tau_{h_{\text{SHK1}}} = a$ $I_{\text{SHK1}} = \bar{g}_{\text{SHK1}} \cdot m_{\text{SHK1}} \cdot h_{\text{SHK1}} \cdot (V - V_K)$

KQT3	$m_{\text{KQT3},\infty}^f(V) = m_{\text{KQT3},\infty}^s(V) = \frac{1}{1 + e^{\frac{-(V-V_{0.5})}{k_a}}}$ $\tau_{m_{\text{KQT3}}}^f(V) = \frac{a}{1 + \left(\frac{V+b}{c}\right)^2}$ $\tau_{m_{\text{KQT3}}}^s(V) = a + \frac{b}{1 + 10^{-c(d-V)}} + \frac{\tilde{e}}{1 + 10^{-f(g+V)}}$ $w_{\text{KQT3},\infty}(V) = s_{\text{KQT3},\infty}(V) = a + \frac{b}{1 + e^{\frac{(V-V_{0.5})}{k_i}}}$ $\tau_{w_{\text{KQT3}}}(V) = a + \frac{b}{1 + \left(\frac{V-c}{d}\right)^2}$ $\tau_{s_{\text{KQT3}}}(V) = a$ $I_{\text{KQT3}} = \bar{g}_{\text{KQT3}} \cdot (0.7m_{\text{KQT3}}^f + 0.3m_{\text{KQT3}}^s) \cdot w_{\text{KQT3}} \cdot s_{\text{KQT3}} \cdot (V - V_K)$
EGL2	$m_{\text{EGL2},\infty}(V) = \frac{1}{1 + e^{\frac{-(V-V_{0.5})}{k_a}}}$ $\tau_{m_{\text{EGL2}}}(V) = \frac{a}{1 + e^{\frac{(V-b)}{c}}} + d$ $I_{\text{EGL2}} = \bar{g}_{\text{EGL2}} \cdot m_{\text{EGL2}} \cdot (V - V_K)$
EGL36	$m_{\text{EGL36},\infty}^f(V) = m_{\text{EGL36},\infty}^m(V) = m_{\text{EGL36},\infty}^s(V) = \frac{1}{1 + e^{\frac{-(V-V_{0.5})}{k_a}}}$ $\tau_{m_{\text{EGL36}}}^f = \tau_{m_{\text{EGL36}}}^m = \tau_{m_{\text{EGL36}}}^s = a$ $I_{\text{EGL36}} = \bar{g}_{\text{EGL36}} \cdot (0.33m_{\text{EGL36}}^f + 0.36m_{\text{EGL36}}^m + 0.39m_{\text{EGL36}}^s) \cdot (V - V_K)$
IRK	$m_{\text{IRK},\infty}(V) = \frac{1}{1 + e^{\frac{(V-V_{0.5})}{k_a}}}$ $\tau_{m_{\text{IRK}}}(V) = \frac{a}{e^{\frac{-(V-b)}{c}} + e^{\frac{(V-d)}{\tilde{e}}}} + f$ $I_{\text{IRK}} = \bar{g}_{\text{IRK}} \cdot m_{\text{IRK}} \cdot (V - V_K)$
EGL19	$m_{\text{EGL19},\infty}(V) = \frac{1}{1 + e^{\frac{-(V-V_{0.5})}{k_a}}}$ $\tau_{m_{\text{EGL19}}}(V) = \left[ae^{-\left(\frac{V-b}{c}\right)^2}\right] + \left[de^{-\left(\frac{V-\tilde{e}}{f}\right)^2}\right] + g$ $h_{\text{EGL19},\infty}(V) = \left[\frac{a}{1 + e^{\frac{-(V-V_{0.5})}{k_i}}} + b\right] \cdot \left[\frac{c}{1 + e^{\frac{(V-V_{0.5}^b)}{k_i^b}}} + d\right]$ $\tau_{h_{\text{EGL19}}}(V) = a \left[\frac{b}{1 + e^{\frac{(V-c)}{d}}} + \frac{\tilde{e}}{1 + e^{\frac{(V-f)}{g}}} + h\right]$ $I_{\text{EGL19}} = \bar{g}_{\text{EGL19}} \cdot m_{\text{EGL19}} \cdot h_{\text{EGL19}} \cdot (V - V_{Ca})$

UNC2	$m_{\text{UNC2},\infty}(V) = \frac{1}{1 + e^{\frac{-(V-V_{0.5})}{k_a}}}$ $\tau_{m_{\text{UNC2}}}(V) = \frac{a}{e^{\frac{-(V-b)}{c}} + e^{\frac{(V-b)}{d}}} + \tilde{\epsilon}$ $h_{\text{UNC2},\infty}(V) = \frac{1}{1 + e^{\frac{(V-V_{0.5})}{k_i}}}$ $\tau_{h_{\text{UNC2}}}(V) = \frac{a}{1 + e^{\frac{-(V-b)}{c}}} + \frac{d}{1 + e^{\frac{(V-\tilde{\epsilon})}{f}}}$ $I_{\text{UNC2}} = \bar{g}_{\text{UNC2}} \cdot m_{\text{UNC2}} \cdot h_{\text{UNC2}} \cdot (V - V_{Ca})$
CCA1	$m_{\text{CCA1},\infty}(V) = \frac{1}{1 + e^{\frac{-(V-V_{0.5})}{k_a}}}$ $h_{\text{CCA1},\infty}(V) = \frac{1}{1 + e^{\frac{(V-V_{0.5})}{k_i}}}$ $\tau_{m_{\text{CCA1}}}(V) = \frac{a}{1 + e^{\frac{-(V-b)}{c}}} + d$ $\tau_{h_{\text{CCA1}}}(V) = \frac{a}{1 + e^{\frac{(V-b)}{c}}} + d$ $I_{\text{CCA1}} = \bar{g}_{\text{CCA1}} \cdot m_{\text{CCA1}}^2 \cdot h_{\text{CCA1}} \cdot (V - V_{Ca})$
SLO1_UNC2	$m_{\text{BK},\infty}(V, Ca) = \frac{m_{\text{CaV}} k_o^+ (\alpha + \beta + k_c^-)}{(k_o^+ + k_o^-)(k_c^- + \alpha) + \beta k_c^-}$ $\tau_{m_{\text{BK}}}(V, Ca) = \frac{\alpha + \beta + k_c^-}{(k_o^+ + k_o^-)(k_c^- + \alpha) + \beta k_c^-}$ $\alpha = \frac{m_{\text{CaV},\infty}}{\tau_{m_{\text{CaV}}}}$ $\beta = \tau_{m_{\text{CaV}}}^{-1} - \alpha$ $I_{\text{BK}} = \bar{g}_{\text{BK}} \cdot m_{\text{BK}} \cdot h_{\text{CaV}} \cdot (V - V_K)$
SLO1_EGL19	$m_{\text{BK},\infty}(V, Ca) = \frac{m_{\text{CaV}} k_o^+ (\alpha + \beta + k_c^-)}{(k_o^+ + k_o^-)(k_c^- + \alpha) + \beta k_c^-}$ $\tau_{m_{\text{BK}}}(V, Ca) = \frac{\alpha + \beta + k_c^-}{(k_o^+ + k_o^-)(k_c^- + \alpha) + \beta k_c^-}$ $\alpha = \frac{m_{\text{CaV},\infty}}{\tau_{m_{\text{CaV}}}}$ $\beta = \tau_{m_{\text{CaV}}}^{-1} - \alpha$ $I_{\text{BK}} = \bar{g}_{\text{BK}} \cdot m_{\text{BK}} \cdot h_{\text{CaV}} \cdot (V - V_K)$
SLO2_UNC2	$m_{\text{BK},\infty}(V, Ca) = \frac{m_{\text{CaV}} k_o^+ (\alpha + \beta + k_c^-)}{(k_o^+ + k_o^-)(k_c^- + \alpha) + \beta k_c^-}$ $\tau_{m_{\text{BK}}}(V, Ca) = \frac{\alpha + \beta + k_c^-}{(k_o^+ + k_o^-)(k_c^- + \alpha) + \beta k_c^-}$ $\alpha = \frac{m_{\text{CaV},\infty}}{\tau_{m_{\text{CaV}}}}$ $\beta = \tau_{m_{\text{CaV}}}^{-1} - \alpha$ $I_{\text{BK}} = \bar{g}_{\text{BK}} \cdot m_{\text{BK}} \cdot h_{\text{CaV}} \cdot (V - V_K)$

SLO2_EGL19	$m_{\text{BK},\infty}(V, Ca) = \frac{m_{\text{CaV}} k_o^+ (\alpha + \beta + k_c^-)}{(k_o^+ + k_o^-)(k_c^- + \alpha) + \beta k_c^-}$ $\tau_{m_{\text{BK}}}(V, Ca) = \frac{\alpha + \beta + k_c^-}{(k_o^+ + k_o^-)(k_c^- + \alpha) + \beta k_c^-}$ $\alpha = \frac{m_{\text{CaV},\infty}}{\tau_{m_{\text{CaV}}}}$ $\beta = \tau_{m_{\text{CaV}}}^{-1} - \alpha$ $I_{\text{BK}} = \bar{g}_{\text{BK}} \cdot m_{\text{BK}} \cdot h_{\text{CaV}} \cdot (V - V_K)$
KCNL	$m_{\text{KCNL},\infty}(Ca) = \frac{Ca}{K_{Ca} + Ca}$ $\tau_{m_{\text{KCNL}}} = a$ $I_{\text{KCNL}} = \bar{g}_{\text{KCNL}} \cdot m_{\text{KCNL}} \cdot (V - V_K)$
NCA	$I_{NCA} = \bar{g}_{NCA} \cdot (V - V_{Na})$

Supplementary Table 2. Ion Channel Model Parameters

Ion Channel	Function	Parameter	Value	Unit
SHL1	m_∞	$V_{0.5}$	11	mV
		k_a	14.1	mV
	h_∞	$V_{0.5}$	-33.1	mV
		k_i	8.3	mV
	τ_m	a	13.8	ms
		b	-17.5	mV
		c	12.9	mV
		d	-3.7	mV
		e	6.5	mV
		f	1.9	ms
	τ_h^f	a	539.2	ms
		b	-28.2	mV
		c	4.9	mV
		d	27.3	ms
	τ_h^s	a	8422	ms
		b	-37.7	mV
		c	6.4	mV
		d	118.9	ms
SHK1	m_∞	$V_{0.5}$	20.4	mV
		k_a	7.7	mV
	h_∞	$V_{0.5}$	-7	mV
		k_i	5.8	mV
	τ_m	a	26.6	ms
		b	-33.7	mV
		c	15.8	mV
		d	-33.7	mV
		e	15.4	mV
		f	2	ms
	τ_h	a	1400	ms
KVS1	m_∞	$V_{0.5}$	57.1	mV
		k_a	25	mV
	h_∞	$V_{0.5}$	47	mV
		k_i	11.1	mV
	τ_m	a	30	ms
		b	18.1	mV
		c	20	mV
		d	1	ms
	τ_h^f	a	88.5	ms
		b	50	mV

		c	-15	mV
		d	53.4	ms
KQT3	m_∞	$V_{0.5}$	-12.6726	mV
		k_a	15.8008	mV
	w_∞	$V_{0.5}$	-1.084	mV
		k_i	28.78	mV
		a	0.49	
		b	0.51	
	s_∞	$V_{0.5}$	-45.3	mV
		k_i	12.3	mV
		a	0.34	
		b	0.66	
	τ_m^f	a	395.3	ms
		b	38.1	mV
		c	33.59	mV
	τ_m^s	a	5503	ms
		b	-5345.4	ms
		c	0.02827	mV^{-1}
		d	-23.9	mV
		e	4590.6	ms
		f	0.0357	mV^{-1}
		g	14.15	mV
	τ_w	a	0.544	ms
		b	29.2	ms
		c	-48.09	mV
		d	48.83	mV
	τ_s	a	500000	ms
EGL2	m_∞	$V_{0.5}$	-6.9	mV
		k_a	14.9	mV
	τ_m	a	1845.8	ms
		b	-122.6	mV
		c	-13.8	mV
		d	1517.74	ms
EGL36	m_∞	$V_{0.5}$	63	mV
		k_a	28.5	mV
	τ_m^s	a	355	ms
	τ_m^m	a	63	ms
IRK	τ_m^f	a	13	ms
	m_∞	$V_{0.5}$	-82	mV
		k_a	13	mV
	τ_m	a	17.1	ms
		b	-17.8	mV

		c	20.3	mV
		d	-43.4	mV
		e	11.2	mV
		f	3.8	ms
EGL19	m_∞	$V_{0.5}$	5.6	mV
		k_a	7.5	mV
	h_∞	$V_{0.5}^b$	24.9	mV
		k_i^b	12	mV
		$V_{0.5}^{b^b}$	-20.5	mV
		$k_i^{b^b}$	8.1	mV
		a	1.43	
		b	0.14	
	τ_m	c	5.96	
		d	0.6	
		a	2.9	ms
		b	5.2	mV
		c	6	mV
		d	1.9	ms
		e	1.4	mV
UNC2	τ_h	f	30	mV
		g	2.3	ms
		a	0.4	
		b	44.6	ms
		c	-23	mV
		d	5	mV
		e	36.4	ms
		f	28.7	mV
	m_∞	g	3.7	mV
		h	43.1	ms
UNC2	m_∞	$V_{0.5}$	-12.2	mV
		k_a	4	mV
	h_∞	$V_{0.5}$	-52.5	mV
		k_i	5.6	mV
	τ_m	a	1.5	ms
		b	-8.2	mV
		c	9.1	mV
		d	15.4	mV
		e	0.1	ms
	τ_h	a	83.8	ms
		b	52.9	mV
		c	-3.5	mV
		d	72.1	ms

		e	23.9	mV
		f	-3.6	mV
CCA1	m_∞	$V_{0.5}$	-43.32	mV
		k_a	7.6	mV
	h_∞	$V_{0.5}$	-58	mV
		k_i	7	mV
	τ_m	a	40	ms
		b	-62.5	mV
		c	-12.6	mV
		d	0.7	ms
	τ_h	a	280	ms
		b	-60.7	mV
		c	8.5	mV
		d	19.8	ms
SLO1	w_{yx}		0.013	mV^{-1}
	w_{xy}		-0.028	mV^{-1}
	w_θ^-		3.15	ms^{-1}
	w_θ^+		0.16	ms^{-1}
	K_{xy}		55.73	$\mu\text{M}/\mu\text{m}^3$
	n_{xy}		1.3	
	K_{yx}		34.34	$\mu\text{M}/\mu\text{m}^3$
	n_{yx}		10-4	
SLO2	w_{yx}		0.019	mV^{-1}
	w_{xy}		-0.024	mV^{-1}
	w_θ^-		0.9	ms^{-1}
	w_θ^+		0.027	ms^{-1}
	K_{xy}		93.45	$\mu\text{M}/\mu\text{m}^3$
	n_{xy}		1.84	
	K_{yx}		3294.55	$\mu\text{M}/\mu\text{m}^3$
	n_{yx}		10-5	
KCNL	K_{Ca}		0.33	μM
	τ_m	a	6.3	ms
Intracellular calcium calculation	g_{sc}		40	pS
	V_{Ca}		60	mV
	r		13	nm
	F		96485	C mol^{-1}
	D_{Ca}		250	$\mu\text{m}^2/\text{s}$
	k_B^+		500	$\mu\text{M}^{-1} \text{ s}^{-1}$
	$[B]_{\text{tot}}$		30	μM
	$[\text{Ca}^{2+}]_{c,i}^n$		0.05	μM
	V_{cell}		31.63	μm^3
	f		0.001	

	τ_{Ca} $[Ca^{2+}]_{eq}^m$	50 0.05	ms $\mu M/\mu m^2$
--	-----------------------------------	------------	-----------------------

Supplementary Table 3. Neuron Model Parameters

Parameters	AWC	AIY	RIM	VD5	AVA
R_a ($\Omega \cdot cm$)	380	269	344	221	150
C_m ($\mu F/cm^2$)	2	7	4	2	8
g_{pas} (S/cm^2)	0.00003	0.000014	0.000077	0.00005	0.00007
R_m ($k\Omega \cdot cm^2$)	33.3	71.4	13	20	14.3
e_{pas} (mV)	-65	-54.5	-33	-75	-33
\bar{g}_{SHL1} ($nS/\mu m^2$)	0.0026	0.001	0.001	0.001	0.0004
\bar{g}_{SHK1} ($nS/\mu m^2$)	0	0.00047	0.00015	0.0055	0.001
\bar{g}_{KVS1} ($nS/\mu m^2$)	0	0.0005	0.0001	0	0
\bar{g}_{EGL2} ($nS/\mu m^2$)	0	0.001	0.00001	0.001	0
\bar{g}_{EGL36} ($nS/\mu m^2$)	0	0.00049	0.0012	0.0046	0
\bar{g}_{KQT3} ($nS/\mu m^2$)	0.022	0.0005	0.00005	0.00016	0
\bar{g}_{EGL19} ($nS/\mu m^2$)	0.006	0.0001	0	0.0001	0.002
\bar{g}_{UNC2} ($nS/\mu m^2$)	0.001	0	0	0	0.0001
\bar{g}_{CCA1} ($nS/\mu m^2$)	0	0.00017	0	0.0015	0.0006
\bar{g}_{SLO1_EGL19} ($nS/\mu m^2$)	0	0.00028	0.000013	0	0
\bar{g}_{SLO1_UNC2} ($nS/\mu m^2$)	0	0.000174	0.009	0.004	0.06
\bar{g}_{SLO2_EGL19} ($nS/\mu m^2$)	0	0.0015	0.00067	0.0013	0
\bar{g}_{SLO2_UNC2} ($nS/\mu m^2$)	0	0.0022	0	0.0006	0
\bar{g}_{KCNL} ($nS/\mu m^2$)	0	0.00063	0	0	0.005
\bar{g}_{NCA} ($nS/\mu m^2$)	0	0.000085	0	0.00015	0.0007
\bar{g}_{IRK} ($nS/\mu m^2$)	0	0.0011	0.00105	0	0

Supplementary Table 4. 302 Neurons and Functional Groups

Index	Neuron	Functional Group	Parameter Reference
1	I1L	interneuron	AIY
2	I1R	interneuron	AIY
3	I2L	interneuron	AIY
4	I2R	interneuron	AIY
5	I3	interneuron	AIY
6	I4	interneuron	AIY
7	I5	interneuron	AIY
8	I6	interneuron	AIY
9	M1	body motor neuron	VD5
10	M2L	body motor neuron	VD5
11	M2R	body motor neuron	VD5
12	M3L	body motor neuron	VD5
13	M3R	body motor neuron	VD5
14	M4	body motor neuron	VD5
15	M5	body motor neuron	VD5
16	MCL	body motor neuron	VD5
17	MCR	body motor neuron	VD5
18	MI	body motor neuron	VD5
19	NSML	interneuron	AIY
20	NSMR	interneuron	AIY
21	ASIL	sensory neuron	AWC
22	ASIR	sensory neuron	AWC
23	ASJL	sensory neuron	AWC
24	ASJR	sensory neuron	AWC
25	AWAL	sensory neuron	AWC
26	AWAR	sensory neuron	AWC
27	ASGL	sensory neuron	AWC
28	ASGR	sensory neuron	AWC
29	AWBL	sensory neuron	AWC
30	AWBR	sensory neuron	AWC
31	ASEL	sensory neuron	AWC
32	ASER	sensory neuron	AWC
33	ADFL	sensory neuron	AWC
34	ADFR	sensory neuron	AWC
35	AFDL	sensory neuron	AWC
36	AFDR	sensory neuron	AWC
37	AWCL	sensory neuron	AWC
38	AWCR	sensory neuron	AWC
39	ASKL	sensory neuron	AWC
40	ASKR	sensory neuron	AWC

41	ASHL	sensory neuron	AWC
42	ASHR	sensory neuron	AWC
43	ADLL	sensory neuron	AWC
44	ADLR	sensory neuron	AWC
45	BAGL	sensory neuron	AWC
46	BAGR	sensory neuron	AWC
47	URXL	sensory neuron	AWC
48	URXR	sensory neuron	AWC
49	ALNL	sensory neuron	AWC
50	ALNR	sensory neuron	AWC
51	PLNL	sensory neuron	AWC
52	PLNR	sensory neuron	AWC
53	SDQL	sensory neuron	AWC
54	SDQR	sensory neuron	AWC
55	AQR	sensory neuron	AWC
56	PQR	sensory neuron	AWC
57	ALML	sensory neuron	AWC
58	ALMR	sensory neuron	AWC
59	AVM	sensory neuron	AWC
60	PVM	sensory neuron	AWC
61	PLML	sensory neuron	AWC
62	PLMR	sensory neuron	AWC
63	FLPL	sensory neuron	AWC
64	FLPR	sensory neuron	AWC
65	DVA	interneuron	AIY
66	PVDL	sensory neuron	AWC
67	PVDR	sensory neuron	AWC
68	ADEL	sensory neuron	AWC
69	ADER	sensory neuron	AWC
70	PDEL	sensory neuron	AWC
71	PDER	sensory neuron	AWC
72	PHAL	sensory neuron	AWC
73	PHAR	sensory neuron	AWC
74	PHBL	sensory neuron	AWC
75	PHBR	sensory neuron	AWC
76	PHCL	sensory neuron	AWC
77	PHCR	sensory neuron	AWC
78	IL2DL	sensory neuron	AWC
79	IL2DR	sensory neuron	AWC
80	IL2L	sensory neuron	AWC
81	IL2R	sensory neuron	AWC
82	IL2VL	sensory neuron	AWC
83	IL2VR	sensory neuron	AWC

84	CEPDL	sensory neuron	AWC
85	CEPDR	sensory neuron	AWC
86	CEPVL	sensory neuron	AWC
87	CEPVR	sensory neuron	AWC
88	URYDL	sensory neuron	AWC
89	URYDR	sensory neuron	AWC
90	URYVL	sensory neuron	AWC
91	URYVR	sensory neuron	AWC
92	OLLL	sensory neuron	AWC
93	OLLR	sensory neuron	AWC
94	OLQDL	sensory neuron	AWC
95	OLQDR	sensory neuron	AWC
96	OLQVL	sensory neuron	AWC
97	OLQVR	sensory neuron	AWC
98	IL1DL	sensory neuron	AWC
99	IL1DR	sensory neuron	AWC
100	IL1L	sensory neuron	AWC
101	IL1R	sensory neuron	AWC
102	IL1VL	sensory neuron	AWC
103	IL1VR	sensory neuron	AWC
104	AINL	interneuron	AIY
105	AINR	interneuron	AIY
106	AIML	interneuron	AIY
107	AIMR	interneuron	AIY
108	RIH	interneuron	AIY
109	URBL	interneuron	AIY
110	URBR	interneuron	AIY
111	RIR	interneuron	AIY
112	AIYL	interneuron	AIY
113	AIYR	interneuron	AIY
114	AIAL	interneuron	AIY
115	AIAR	interneuron	AIY
116	AUAL	interneuron	AIY
117	AUAR	interneuron	AIY
118	AIZL	interneuron	AIY
119	AIZR	interneuron	AIY
120	RIS	interneuron	AIY
121	ALA	interneuron	AIY
122	PVQL	interneuron	AIY
123	PVQR	interneuron	AIY
124	ADAL	interneuron	AIY
125	ADAR	interneuron	AIY
126	RIFL	interneuron	AIY

127	RIFR	interneuron	AIY
128	BDUL	interneuron	AIY
129	BDUR	interneuron	AIY
130	PVR	interneuron	AIY
131	AVFL	interneuron	AIY
132	AVFR	interneuron	AIY
133	AVHL	interneuron	AIY
134	AVHR	interneuron	AIY
135	PVPL	interneuron	AIY
136	PVPR	interneuron	AIY
137	LUAL	interneuron	AIY
138	LUAR	interneuron	AIY
139	PVNL	interneuron	AIY
140	PVNR	interneuron	AIY
141	AVG	interneuron	AIY
142	DVB	interneuron	AIY
143	RIBL	interneuron	AIY
144	RIBR	interneuron	AIY
145	RIGL	interneuron	AIY
146	RIGR	interneuron	AIY
147	RMGL	head motor neuron	RIM
148	RMGR	head motor neuron	RIM
149	AIBL	interneuron	AIY
150	AIBR	interneuron	AIY
151	RICL	interneuron	AIY
152	RICR	interneuron	AIY
153	SAADL	interneuron	AIY
154	SAADR	interneuron	AIY
155	SAAVL	interneuron	AIY
156	SAAVR	interneuron	AIY
157	AVKL	interneuron	AIY
158	AVKR	interneuron	AIY
159	DVC	interneuron	AIY
160	AVJL	interneuron	AIY
161	AVJR	interneuron	AIY
162	PVT	interneuron	AIY
163	AVDL	interneuron	AIY
164	AVDR	interneuron	AIY
165	AVL	interneuron	AIY
166	PVWL	interneuron	AIY
167	PVWR	interneuron	AIY
168	RIAL	interneuron	AIY
169	RIAR	interneuron	AIY

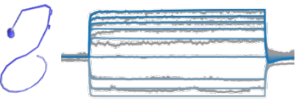
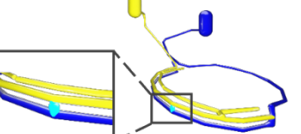
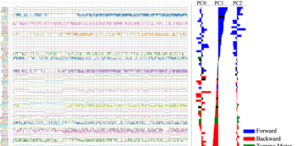
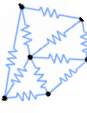
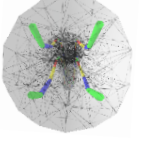
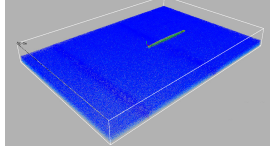
170	RIML	head motor neuron	RIM
171	RIMR	head motor neuron	RIM
172	AVEL	command neuron	AVA
173	AVER	command neuron	AVA
174	RMFL	head motor neuron	RIM
175	RMFR	head motor neuron	RIM
176	RID	interneuron	AIY
177	AVBL	command neuron	AVA
178	AVBR	command neuron	AVA
179	AVAL	command neuron	AVA
180	AVAR	command neuron	AVA
181	PVCL	command neuron	AVA
182	PVCR	command neuron	AVA
183	RIPL	interneuron	AIY
184	RIPR	interneuron	AIY
185	URADL	head motor neuron	RIM
186	URADR	head motor neuron	RIM
187	URAVL	head motor neuron	RIM
188	URAVR	head motor neuron	RIM
189	RMEL	head motor neuron	RIM
190	RMER	head motor neuron	RIM
191	RMED	head motor neuron	RIM
192	RMEV	head motor neuron	RIM
193	RMDDL	head motor neuron	RIM
194	RMDDR	head motor neuron	RIM
195	RMDL	head motor neuron	RIM
196	RMDR	head motor neuron	RIM
197	RMDVL	head motor neuron	RIM
198	RMDVR	head motor neuron	RIM
199	RIVL	head motor neuron	RIM
200	RIVR	head motor neuron	RIM
201	RMHL	head motor neuron	RIM
202	RMHR	head motor neuron	RIM
203	SABD	head motor neuron	RIM
204	SABVL	head motor neuron	RIM
205	SABVR	head motor neuron	RIM
206	SMDDL	head motor neuron	RIM
207	SMDDR	head motor neuron	RIM
208	SMDVL	head motor neuron	RIM
209	SMDVR	head motor neuron	RIM
210	SMBDL	head motor neuron	RIM
211	SMBDR	head motor neuron	RIM
212	SMBVL	head motor neuron	RIM

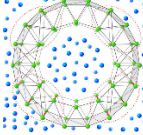
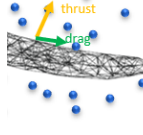
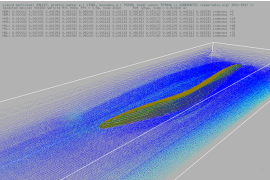
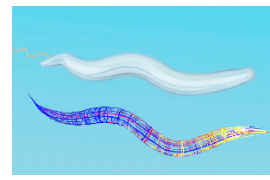
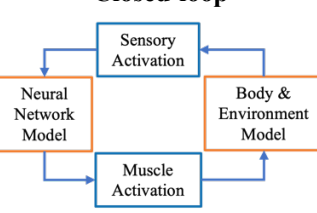
213	SMBVR	head motor neuron	RIM
214	SIBDL	head motor neuron	RIM
215	SIBDR	head motor neuron	RIM
216	SIBVL	head motor neuron	RIM
217	SIBVR	head motor neuron	RIM
218	SIADL	head motor neuron	RIM
219	SIADR	head motor neuron	RIM
220	SIAVL	head motor neuron	RIM
221	SIAVR	head motor neuron	RIM
222	DA1	body motor neuron	VD5
223	DA2	body motor neuron	VD5
224	DA3	body motor neuron	VD5
225	DA4	body motor neuron	VD5
226	DA5	body motor neuron	VD5
227	DA6	body motor neuron	VD5
228	DA7	body motor neuron	VD5
229	DA8	body motor neuron	VD5
230	DA9	body motor neuron	VD5
231	PDA	body motor neuron	VD5
232	DB1	body motor neuron	VD5
233	DB2	body motor neuron	VD5
234	DB3	body motor neuron	VD5
235	DB4	body motor neuron	VD5
236	DB5	body motor neuron	VD5
237	DB6	body motor neuron	VD5
238	DB7	body motor neuron	VD5
239	AS1	body motor neuron	VD5
240	AS2	body motor neuron	VD5
241	AS3	body motor neuron	VD5
242	AS4	body motor neuron	VD5
243	AS5	body motor neuron	VD5
244	AS6	body motor neuron	VD5
245	AS7	body motor neuron	VD5
246	AS8	body motor neuron	VD5
247	AS9	body motor neuron	VD5
248	AS10	body motor neuron	VD5
249	AS11	body motor neuron	VD5
250	PDB	body motor neuron	VD5
251	DD1	body motor neuron	VD5
252	DD2	body motor neuron	VD5
253	DD3	body motor neuron	VD5
254	DD4	body motor neuron	VD5
255	DD5	body motor neuron	VD5

256	DD6	body motor neuron	VD5
257	VA1	body motor neuron	VD5
258	VA2	body motor neuron	VD5
259	VA3	body motor neuron	VD5
260	VA4	body motor neuron	VD5
261	VA5	body motor neuron	VD5
262	VA6	body motor neuron	VD5
263	VA7	body motor neuron	VD5
264	VA8	body motor neuron	VD5
265	VA9	body motor neuron	VD5
266	VA10	body motor neuron	VD5
267	VA11	body motor neuron	VD5
268	VA12	body motor neuron	VD5
269	VB1	body motor neuron	VD5
270	VB2	body motor neuron	VD5
271	VB3	body motor neuron	VD5
272	VB4	body motor neuron	VD5
273	VB5	body motor neuron	VD5
274	VB6	body motor neuron	VD5
275	VB7	body motor neuron	VD5
276	VB8	body motor neuron	VD5
277	VB9	body motor neuron	VD5
278	VB10	body motor neuron	VD5
279	VB11	body motor neuron	VD5
280	VD1	body motor neuron	VD5
281	VD2	body motor neuron	VD5
282	VD3	body motor neuron	VD5
283	VD4	body motor neuron	VD5
284	VD5	body motor neuron	VD5
285	VD6	body motor neuron	VD5
286	VD7	body motor neuron	VD5
287	VD8	body motor neuron	VD5
288	VD9	body motor neuron	VD5
289	VD10	body motor neuron	VD5
290	VD11	body motor neuron	VD5
291	VD12	body motor neuron	VD5
292	VD13	body motor neuron	VD5
293	CANL	interneuron	AIY
294	CANR	interneuron	AIY
295	HSNL	body motor neuron	VD5
296	HSNR	body motor neuron	VD5
297	VC1	body motor neuron	VD5
298	VC2	body motor neuron	VD5

299	VC3	body motor neuron	VD5
300	VC4	body motor neuron	VD5
301	VC5	body motor neuron	VD5
302	VC6	body motor neuron	VD5

Supplementary Table 5. Comparisons between OpenWorm and BAAIWorm

Category	OpenWorm	BAAIWorm	
Neural Network Modeling	Multi-compartmental single neuron model	Have not fitted the electrophysiological data yet	Fit the electrophysiological data 
	Connections between neurons	On soma	On neurite 
	Multi-compartmental neural network model	Not trained	Trained with experimental data 
Body Modelling	Worm body	~34000-104000 particles with springs between particles 	984 vertices, 3341 tetrahedrons 
	Soft body solver	Mass-Spring model	Projective dynamics
	Actuator	Contractile fibers (muscle springs) 	FEM constraints 
3D Environment	3D scene scale	A simulation box about 1.5-10 worm body length. 	A large open world space about 1200 worm body length and can be even larger. 
	Fluid solver	Smoothed particle hydrodynamics	Simplified hydrodynamics swimming model

			
Simulation Performance	Simulation time step (default)	0.00002 s	0.00417 s
	Simulation time per step (1 worm, 1 CPU core)	0.4-2 s	0.08-0.1 s
Visualization	Primitives & Methods	Particles, line connections 	Real-time mesh rendering Ray tracing (neurons) 
Interaction	Interaction	Open-loop	<p>Closed-loop</p>  <pre> graph TD SA[Sensor Activation] --> NNM[Neural Network Model] NNM --> MA[Muscle Activation] MA --> BEBM[Body & Environment Model] BEBM --> NNM </pre>

*The performance results are evaluated on personal computer with these configurations: Ubuntu 18.04, NVIDIA GeForce RTX 3060, 16 GB RAM, Intel(R) Core(TM) i7-10700K CPU. c302¹ and Sibernetic² in OpenWorm are the latest version from GitHub when this manuscript is submitted.

Comparison with OpenWorm

OpenWorm is a pioneering open science project that has significantly contributed to computational biology by modeling *C. elegans*. While we have used many valuable tools and data from OpenWorm, such as cell model morphology, synaptic dynamic and 3D worm body information, BAAIWorm advances beyond it in several critical aspects:

1. Enhanced Neural Network Model

OpenWorm provides many valuable tools and standards for modeling nervous system, such as ChannelWorm and c302. However, there are several aspects where BAAIWorm provides significant advancements:

- a) Single neuron modeling: c302 provides multi-compartmental neural models with uniform parameters among neurons. BAAIWorm tunes five single neuron models to fit electrophysiological data, ensuring that the models accurately represent realistic dynamics.

- b) Connection specificity: The multi-compartmental neuron models in c302 are connected on soma. BAAIWorm establishes connections on the neurites of neuron models, enhancing the anatomical accuracy of neural connections.
- c) Training: The multi-compartmental neural network models generated by c302 is not trained. Our network model undergoes rigorous training to fit functional maps, capturing more realistic and complex neural dynamics.

2. Enhanced Body and Environmental Modeling

Siberntic is a physical simulator developed for simulations of *C. elegans* physical body dynamics within the OpenWorm Project. Although Siberntic's particle model has advantages in some specific tasks, such as tasks related to pressure computation, BAAIWorm's body & environment model outperforms it in many aspects:

- a) Body modeling Efficiency: The body surface data of BAAIWorm was converted from the body surface of Siberntic. However, our tetrahedron worm body has much less elements compared to Sibernetic's particle body, which results in a huge performance improvement while preserving anatomical authenticity.
- b) 3D environment: By using simplified hydrodynamics, the scale of our 3D simulation scene increases by two orders of magnitude compared to Sibernetic.
- c) Simulation: The utilization of projective dynamics as the deformation solver has greatly reduced the simulation time per iteration step compared to Sibernetic. Moreover, projective dynamics exhibits stability even with large time steps, enabling the use of larger steps to accelerate simulation.
- d) Visualization: BAAIWorm uses real-time mesh rendering and GPU ray tracing techniques, which bring better visual effects while maintaining high performance.

3. Closed-loop Interaction

While OpenWorm connected the c302 neural network and the Sibernetic body model in a Docker simulation stack, the interaction is open-loop without sensory feedback. BAAIWorm makes the interaction closed-loop with sensory feedback. This allows for a more comprehensive understanding of how the worm interacts with its environment, processes sensory information, and executes coordinated movements.

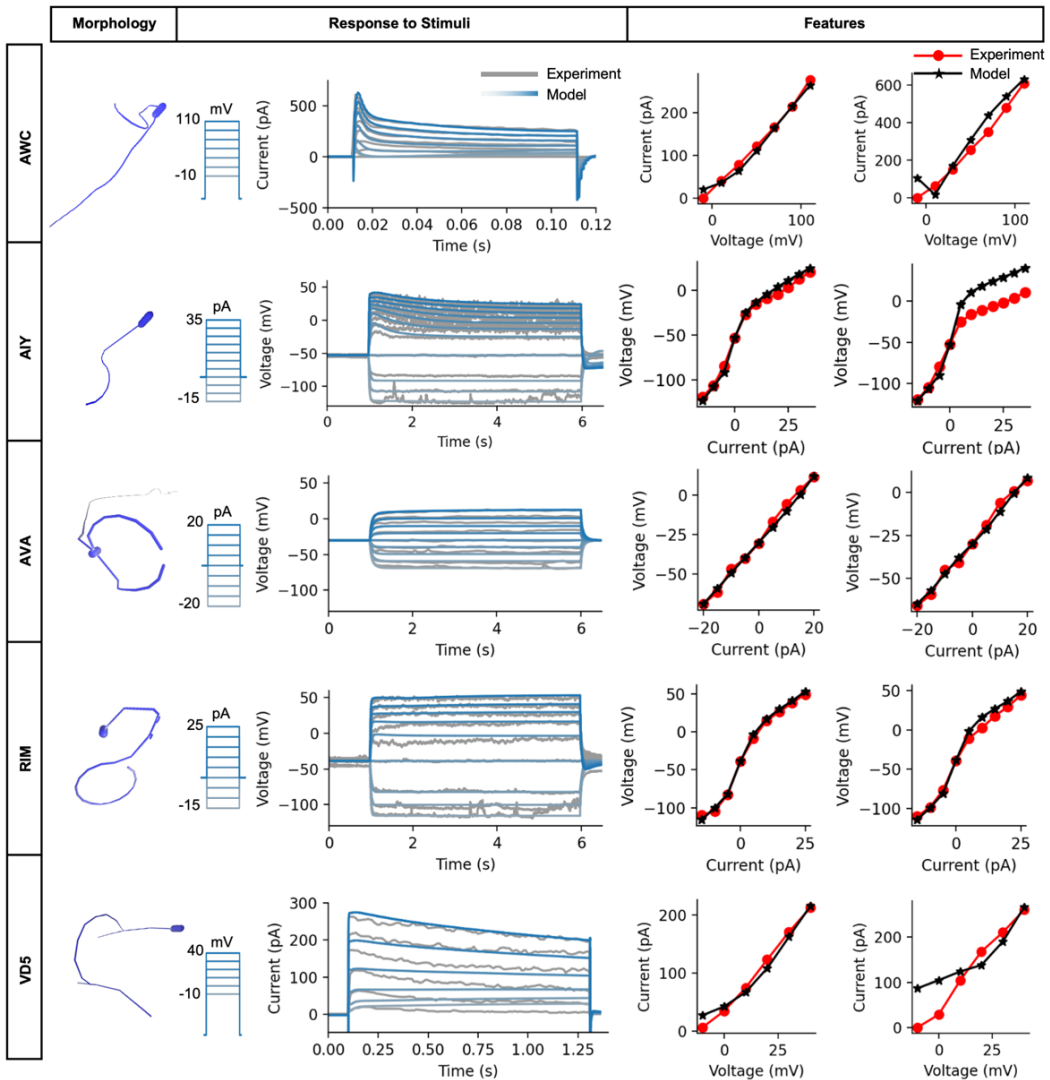
Supplementary Table 6. 136 Neurons Used in Simulation

No.	Index	Neuron	Recorded in Biological Experiment ³	Network Input/Output
1	39	ASKL	yes	input
2	40	ASKR	yes	input
3	49	ALNL	yes	input
4	50	ALNR	yes	input
5	61	PLML	yes	input
6	65	DVA	yes	
7	72	PHAL	yes	input
8	73	PHAR	yes	input
9	88	URYDL	yes	input
10	89	URYDR	yes	input
11	90	URYVL	yes	input
12	91	URYVR	yes	input
13	120	RIS	yes	
14	121	ALA	yes	
15	131	AVFL	yes	
16	132	AVFR	yes	
17	139	PVNL	yes	
18	140	PVNR	yes	
19	142	DVB	yes	
20	143	RIBL	yes	
21	144	RIBR	yes	
22	149	AIBL	yes	
23	150	AIBR	yes	
24	159	DVC	yes	
25	170	RIML	yes	output
26	171	RIMR	yes	output
27	172	AVEL	yes	
28	173	AVER	yes	
29	176	RID	yes	
30	177	AVBL	yes	
31	178	AVBR	yes	
32	179	AVAL	yes	
33	180	AVAR	yes	
34	189	RMEL	yes	output
35	190	RMER	yes	output
36	191	RMED	yes	output
37	192	RMEV	yes	output
38	199	RIVL	yes	output
39	200	RIVR	yes	output

40	203	SABD	yes	
41	204	SABVL	yes	
42	205	SABVR	yes	
43	206	SMDDL	yes	output
44	207	SMDDR	yes	output
45	208	SMDVL	yes	output
46	209	SMDVR	yes	output
47	218	SIADL	yes	
48	219	SIADR	yes	
49	220	SIAVL	yes	
50	221	SIAVR	yes	
51	222	DA1	yes	output
52	228	DA7	yes	output
53	230	DA9	yes	output
54	231	PDA	yes	
55	232	DB1	yes	output
56	233	DB2	yes	output
57	238	DB7	yes	output
58	248	AS10	yes	
59	257	VA1	yes	output
60	267	VA11	yes	output
61	268	VA12	yes	output
62	269	VB1	yes	output
63	270	VB2	yes	output
64	279	VB11	yes	output
65	292	VD13	yes	output
66	25	AWAL	no	input
67	26	AWAR	no	input
68	37	AWCL	no	input
69	38	AWCR	no	input
70	112	AIYL	no	
71	113	AIYR	no	
72	114	AIAL	no	
73	115	AIAR	no	
74	118	AIZL	no	
75	119	AIZR	no	
76	153	SAADL	no	
77	154	SAADR	no	
78	155	SAAVL	no	
79	156	SAAVR	no	
80	181	PVCL	no	
81	182	PVCR	no	
82	193	RMDDL	no	output

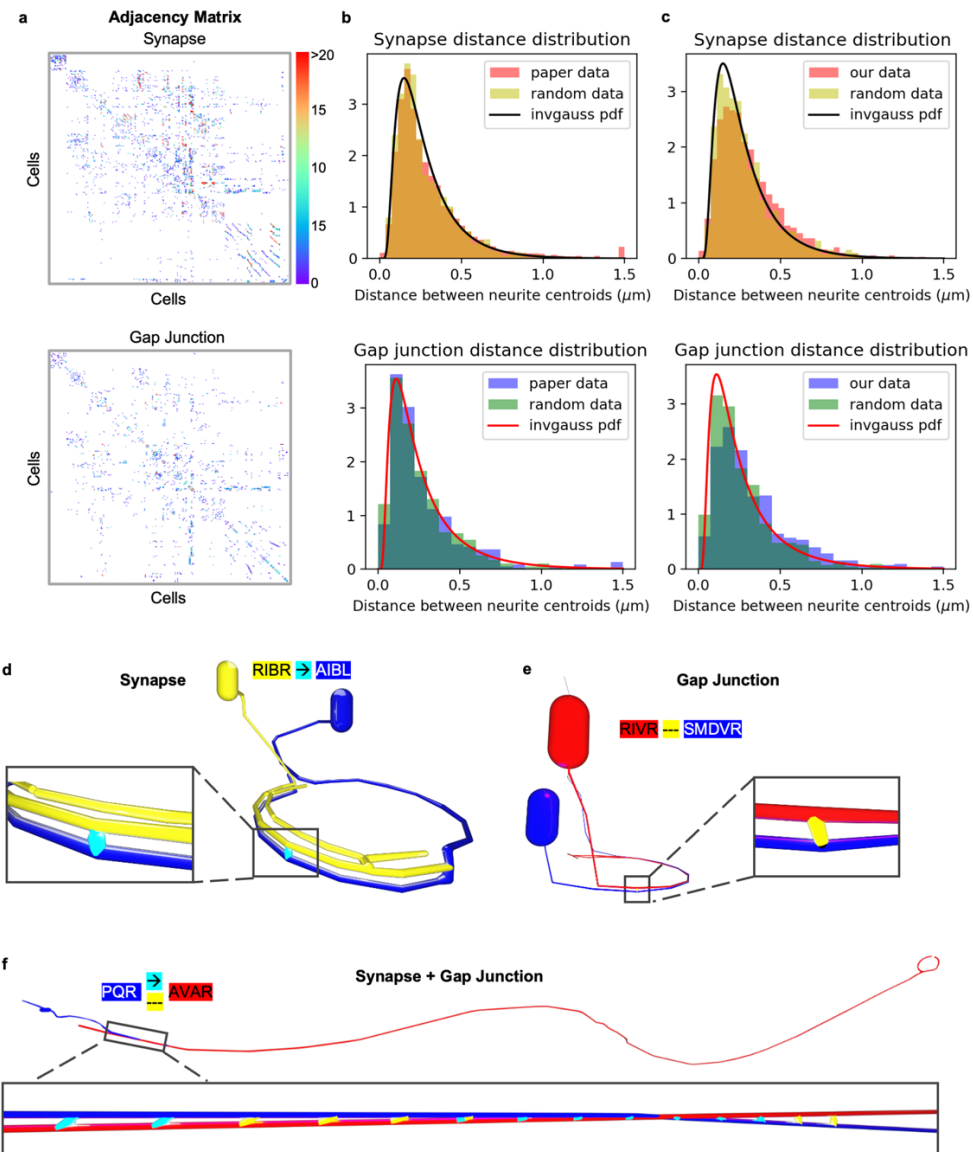
83	194	RMDDR	no	output
84	195	RMDL	no	output
85	196	RMDR	no	output
86	197	RMDVL	no	output
87	198	RMDVR	no	output
88	210	SMBDL	no	output
89	211	SMBDR	no	output
90	212	SMBVL	no	output
91	213	SMBVR	no	output
92	223	DA2	no	output
93	224	DA3	no	output
94	225	DA4	no	output
95	226	DA5	no	output
96	227	DA6	no	output
97	229	DA8	no	output
98	234	DB3	no	output
99	235	DB4	no	output
100	236	DB5	no	output
101	237	DB6	no	output
102	251	DD1	no	output
103	252	DD2	no	output
104	253	DD3	no	output
105	254	DD4	no	output
106	255	DD5	no	output
107	256	DD6	no	output
108	258	VA2	no	output
109	259	VA3	no	output
110	260	VA4	no	output
111	261	VA5	no	output
112	262	VA6	no	output
113	263	VA7	no	output
114	264	VA8	no	output
115	265	VA9	no	output
116	266	VA10	no	output
117	271	VB3	no	output
118	272	VB4	no	output
119	273	VB5	no	output
120	274	VB6	no	output
121	275	VB7	no	output
122	276	VB8	no	output
123	277	VB9	no	output
124	278	VB10	no	output
125	280	VD1	no	output

126	281	VD2	no	output
127	282	VD3	no	output
128	283	VD4	no	output
129	284	VD5	no	output
130	285	VD6	no	output
131	286	VD7	no	output
132	287	VD8	no	output
133	288	VD9	no	output
134	289	VD10	no	output
135	290	VD11	no	output
136	291	VD12	no	output



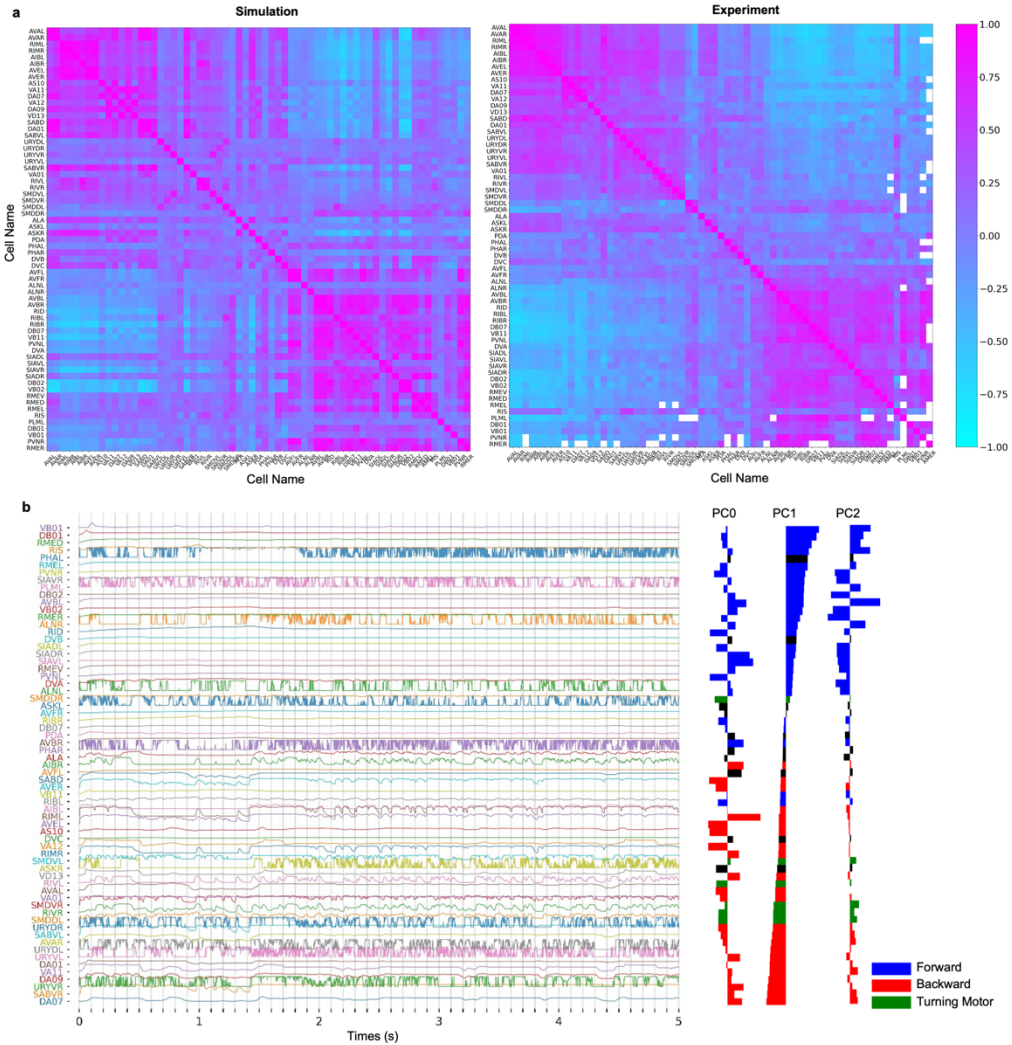
Supplementary Figure 1. Models of five representative neurons fitted to electrophysiological recordings in experiments.

AWC(L), AIY(L), AVA(L), RIM(L), VD5 were selected as the representative neurons for each of the five functional groups, respectively. Left, 3D morphology of each neuron^{1,4}. Middle, membrane voltage/current dynamics induced by current or voltage clamp steps. The simulated responses (blue lines) are overlaid with biological experimental data (gray lines). The corresponding current or voltage clamp protocol are shown in left. AWC(L): voltage clamp protocol, in spans of 0.1 s, starting from -10 mV and increasing to 110 mV by 20 mV increments. AIY(L): current clamp protocol, in spans of 5 s, starting from -15 pA and increasing to 35 pA by 5 pA increments. AVA(L): current clamp protocol, in spans of 5 s, starting from -20 pA and increasing to 20 pA by 5 pA increments. RIM(L): current clamp protocol, in spans of 5 s, starting from -15 pA and increasing to 25 pA by 5 pA increments. VD5: voltage clamp protocol, in spans of 1.2 s, starting from -10 mV and increasing to 40 mV by 10 mV increments. Right, comparison of patch clamp responses features between experimental (red dot) and simulated (black star) I-V curves. The current-voltage relationships at steady-state (left) and at the initial peak point (right) demonstrate the similarity between experimental recordings and our models. Experimental data are from published articles⁵⁻⁸.



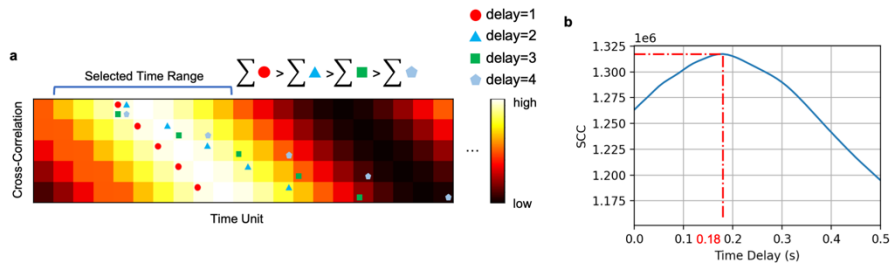
Supplementary Figure 2. Connecting multi-compartmental neuron models in the neural network model.

a. Synapse and gap junction adjacency matrices of the neurons from published data^{9,10}. Matrix elements represent the total number of electron microscopy series capturing synapses (or gap junctions) between two neurons. The color indicates the series number. The order of cells in rows and columns corresponds to Supplementary Table 4. **b.** Distribution of distances between centroids coordinates of neurites at connected synapse (upper) and gap junction (lower) locations. Experimental data (red/blue bars) from a published paper¹¹ is fitted by two inverse Gaussian distributions (black/red lines). Random data (yellow/green bars) is produced following the fitted inverse Gaussian distributions. **c.** Similar to B, with red and blue histograms indicating distributions in our neural network model constructed in our model. **d.** 3D visualization of a synapse (cyan) between RIBR (pre-synaptic, yellow) and AIBL (post-synaptic, blue). **e.** 3D visualization of a gap junction (yellow) between RIVR (red) and SMDVR (blue). **f.** 3D visualization of clusters of synapses (cyan) and gap junctions (yellow) between PQR (blue) and AVAR (red).



Supplementary Figure 3. Neural network model of *C. elegans* fitted to functional map in biological experiment.

a. Pearson correlation matrix of neurons in simulation and experiment³. The simulation matrix was derived from our optimized neural network model. Red and cyan color indicate positive and negative correlation coefficients, which were calculated by membrane potentials of two neurons. **b.** Membrane potentials of 65 neurons, each represented in a separate row. Principal component (PC0, PC1, PC2) weights of each neuron are shown by the bar plots on the right. Neurons were sorted by PC1 weights. Color of the bars indicates the reported role of the neuron in locomotion from published research³ (blue: forward neurons, red: backward neurons, green: turning motor neurons, black: no clear role).



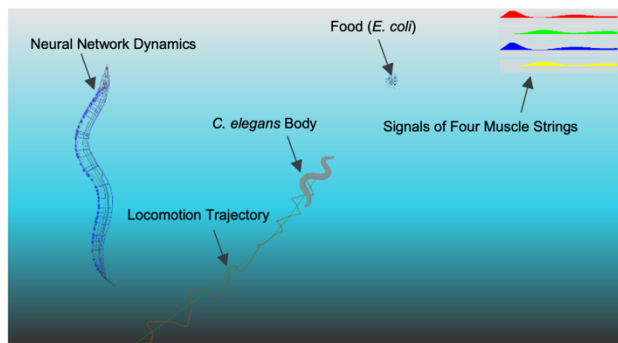
Supplementary Figure 4. The Sum of Cross Correlation (SCC) analysis to imply the muscle activation propagation along the body. **a.** SCC Depiction. Each row represents the cross-correlation between each muscle cell and the reference cell (DR01). SCC of one (two/three/four) time unit(s) delay is the sum of values marked by red circles (blue triangles/green squares/pink pentagons) over the selected time range. **b.** SCC values for different time delays. The largest SCC occurs with a time delay of 0.18 seconds. These SCC values are calculated from the muscle traces of DR01-DR24 in Figure 5e, within the time range of 25-30 seconds.

SCC analysis to imply propagation

To demonstrate that muscle activity propagates along the body, we introduced a measurement named the Sum of Cross-Correlation (SCC). The SCC values with different time delays show significant differences, indicating a traveling wave along the body.

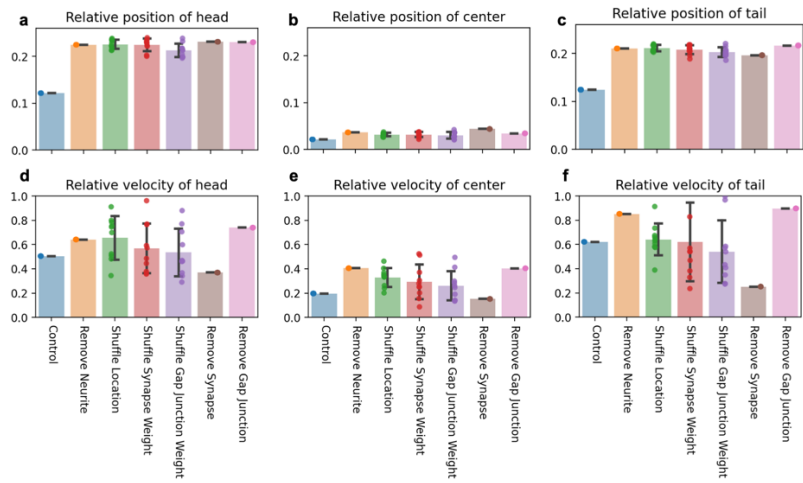
Specifically, we first calculated the cross-correlation between the activities of each muscle cell and the reference cell. Then, we summarized the cross-correlation values with different time delays as SCCs. For example, in Figure S4A, SCC for one time unit delay is the summary of values with red circles over the selected time range (The period where a peak of the reference activation occurs).

If there is an obvious propagation trend, the SCCs will vary significantly with different time delays. The time delay with the largest SCC reflects the propagation velocity. In our model, SCC analysis (Figure S4B) implies a clear traveling wave among the muscles. And with a time delay of 0.18 seconds, SCC is the largest. Given that there are 24 muscle cells from head to tail, it takes approximately 4.32 seconds ($0.18 \text{ seconds} \times 24 \text{ muscles}$) for the wave to propagate from head to tail.

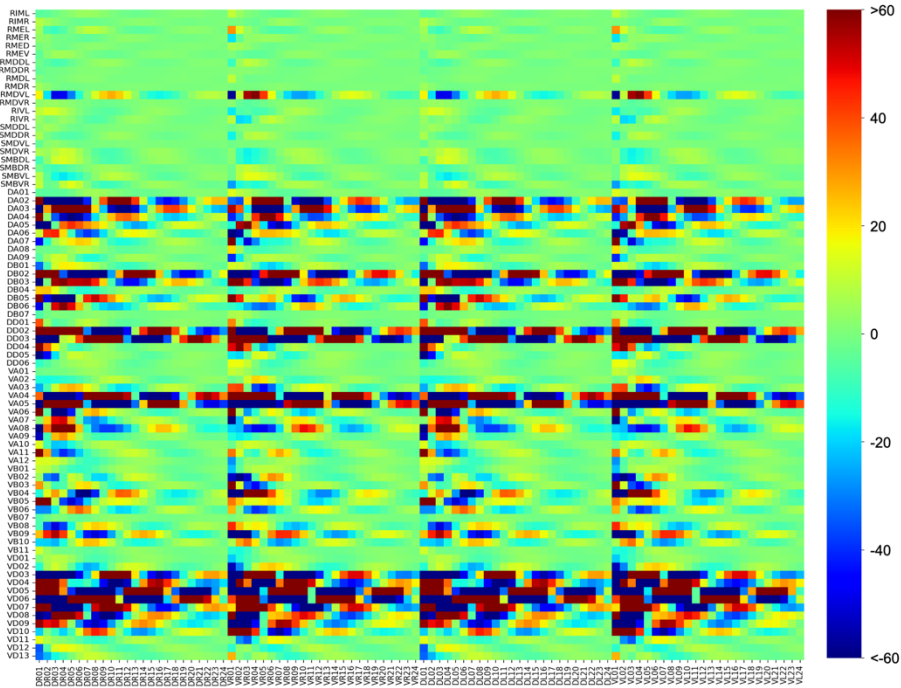


Supplementary Figure 5. Graphical User Interface (GUI) of BAAIWorm.

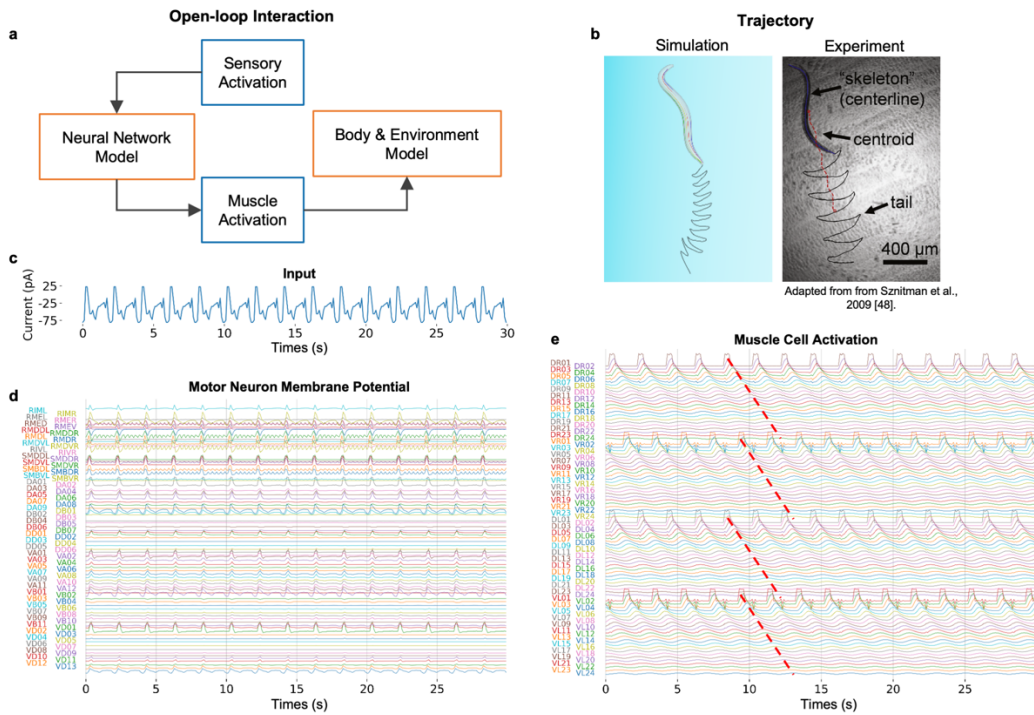
Graphical User Interface (GUI) of BAAIWorm, including: the neural network of *C. elegans* where the color indicates membrane potentials, a *C. elegans* body actively moving towards a food source (*E. coli* population) in the 3D fluid environment, the locomotion trajectory, activations of four muscle strings extending from head to tail.



Supplementary Figure 6. The mean relative position / velocity of tracking points among different simulation trials with different random seeds (n=10). (a-c) The mean relative position of tracking points (Euclidean distance) on head (a), center (b) and tail (c). (d-f) The mean relative velocity of tracking points (Euclidean distance) on head (d), center (e) and tail (f). Each filled circle denotes a value of one random seed. Data are presented as mean values +/- SD.

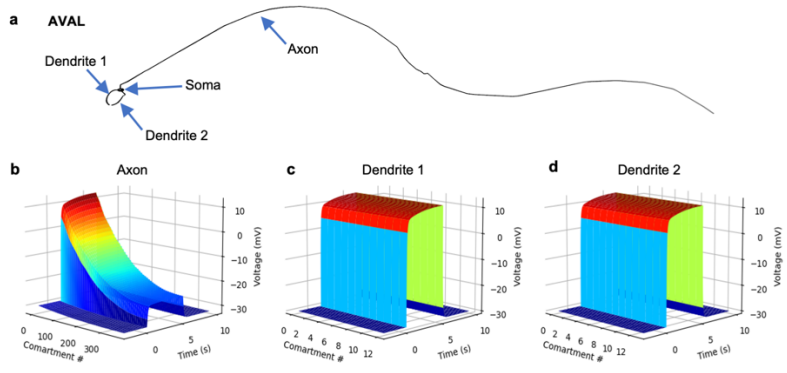


Supplementary Figure 7. The weight matrix (80×96) in our model.



Supplementary Figure 8. The open-loop 3D simulation of *C. elegans* locomotion behavior.

a. The information flow diagram of the open-loop interaction between neural network model and body & environment model. **b.** Comparison of *C. elegans* trajectory during forward locomotion in simulation (left) and experiment (right, from a published article¹²). **c.** Input current injected to sensory neurons during locomotion. **d.** Left, neural network model of *C. elegans*. Right, membrane potentials of all motor neurons in the model during locomotion. **e.** Left, the body model with 96 muscle cells. Right, the activation signals of all muscle cells during locomotion. The dashed red line indicates that the activation signal shifting from head to tail.



Supplementary Figure 9. Membrane potentials of three sections on AVAL.

a. The morphology of AVAL. **b-d.** membrane potential of all compartments on axon (**b**), dendrite 1 (**c**) and dendrite 2 (**d**).

Supplementary Algorithm

Algorithm 1. Generate connection locations.

Input:

- $A\{a_0, a_1, \dots, a_{N_a-1}\}$: set of all compartments of neuron A.
- $B\{b_0, b_1, \dots, b_{N_b-1}\}$: set of all compartments of another neuron B.
- $N_s (N_g)$: desired synapses (gap junctions) number between these two neurons.
- $D_s (D_g)$: Inverse Gaussian distribution of synapses (gap junctions) fitted above.
- d_{th} : distance threshold of one synapse (gap junction).
- ρ : arrangement priority factor between synapse and gap junction.

Output:

$C_s\{(a_{i1}^s, b_{j1}^s), (a_{i2}^s, b_{j2}^s), \dots, (a_{iN}^s, b_{jN}^s)\}$ (C_g): set of synapse (gap junction)

compartments that best approximates D_s (D_g) distribution.

Algorithm:

randomly sample synapses (gap junction) distances $T_s\{t_0^s, t_1^s, \dots, t_{N_s-1}^s\}(T_g)$ according to $D_s(D_g)$.

initialize distance matrix M

```

for  $i = 0 \dots (N_a - 1)$  do
    for  $j = 0 \dots (N_b - 1)$  do
         $M_{i,j} :=$  Euclidean_Distance( $a_i, b_j$ )
    end for
end for
initial index pointer  $ptr_s(ptr_g)$  of synapses (gap junction) allocation status
 $ptr_s := 0$ 
 $ptr_g := 0$ 
while ( $ptr_s < N_s$ ) or ( $ptr_g < N_g$ ) do
    randomly sampled a uniform[0,1] variable  $r$ 

```

```

if  $((r < \rho) \text{ or } (ptr_g == N_g)) \text{ and } (ptr_s < N_s)$  then
    find connection  $(a_p, b_q)$  in distance matrix  $M$  closest to  $t_{ptr_s}^s$ 

```

```

if  $(M_{p,q} < d_{th})$  then
    Append  $(a_p, b_q)$  to  $C_s$ 
     $M_{p,*} := inf$ 
     $M_{q,*} := inf$ 
end if

```

```

 $ptr_s := ptr_s + 1;$ 

```

```

else

```

```

    find connection  $(a_p, b_q)$  in distance matrix  $M$  closest to  $t_{ptr_g}^g$ 

```

```

if  $(M_{p,q} < d_{th})$  then
    Append  $(a_p, b_q)$  to  $C_g$ 
     $M_{p,*} := inf$ 
     $M_{q,*} := inf$ 
end if

```

```

ptrg := ptrg + 1;
end if
end while
return Cs, Cg

```

References

- 1 Gleeson, P., Lung, D., Grosu, R., Hasani, R. & Larson, S. D. c302: a multiscale framework for modelling the nervous system of *< i>Caenorhabditis elegans</i>*. *Philosophical Transactions of the Royal Society B: Biological Sciences* **373**, 20170379 (2018). <https://doi.org/doi:10.1098/rstb.2017.0379>
- 2 Palyanov, A. Y. & Khayrulin, S. S. Sibernetic: A software complex based on the PCI SPH algorithm aimed at simulation problems in biomechanics. *Russian Journal of Genetics: Applied Research* **5**, 635-641 (2015). <https://doi.org/10.1134/S2079059715060052>
- 3 Uzel, K., Kato, S. & Zimmer, M. A set of hub neurons and non-local connectivity features support global brain dynamics in *C. elegans*. *Current Biology* **32**, 3443-3459 (2022). <https://doi.org/https://doi.org/10.1016/j.cub.2022.06.039>
- 4 Grove, C. & Sternberg, P. in *18th International C. elegans Meeting*.
- 5 Liu, Q., Kidd, P. B., Dobosiewicz, M. & Bargmann, C. I. C. elegans AWA Olfactory Neurons Fire Calcium-Mediated All-or-None Action Potentials. *Cell* **175**, 57-70.e17 (2018).
- 6 Mellem, J. E., Brockie, P. J., Madsen, D. M. & Maricq, A. V. Action potentials contribute to neuronal signaling in *C. elegans*. *Nature neuroscience* **11**, 865-867 (2008).
- 7 Liu, P., Chen, B. & Wang, Z.-W. SLO-2 potassium channel is an important regulator of neurotransmitter release in *Caenorhabditis elegans*. *Nature communications* **5**, 5155 (2014).
- 8 Ramot, D., MacInnis, B. L. & Goodman, M. B. Bidirectional temperature-sensing by a single thermosensory neuron in *C. elegans*. *Nature Neuroscience* **11**, 908-915 (2008). <https://doi.org/10.1038/nn.2157>
- 9 White, J. G., Southgate, E., Thomson, J. N. & Brenner, S. The structure of the nervous system of the nematode *Caenorhabditis elegans*. *Philos Trans R Soc Lond B Biol Sci* **314**, 1-340 (1986).
- 10 Cook, S. J. *et al.* Whole-animal connectomes of both *Caenorhabditis elegans* sexes. *Nature* **571**, 63-71 (2019). <https://doi.org/10.1038/s41586-019-1352-7>
- 11 Ruach, R., Ratner, N., Emmons, S. W. & Zaslaver, A. The synaptic organization in the *< i>Caenorhabditis elegans</i>* neural network suggests significant local compartmentalized computations. *Proceedings of the National Academy of Sciences* **120**, e2201699120 (2023). <https://doi.org/doi:10.1073/pnas.2201699120>
- 12 Sznitman, J., Purohit, P. K., Krajacic, P., Lamitina, T. & Arratia, P. E. Material Properties of *< em>Caenorhabditis elegans* Swimming at Low Reynolds Number. *Biophysical Journal* **98**, 617-626 (2010). <https://doi.org/10.1016/j.bpj.2009.11.010>